(12) INTERNATIONAL APPLICATION PUBLISHED UNDER THE PATENT COOPERATION TREATY (PCT)

(19) World Intellectual Property Organization
International Bureau

(43) International Publication Date
04 January 2018 (04.01.2018)

WIPO | PCT

(10) International Publication Number
WO 2018/000294 A1

(51) International Patent Classification:
H01L 31/032 (2006.01) *H01L 31/18* (2006.01)

(21) International Application Number:
PCT/CN2016/087831

(22) International Filing Date:
30 June 2016 (30.06.2016)

(25) Filing Language: English

(26) Publication Language: English

(71) Applicant: **THE UNIVERSITY OF HONG KONG** [CN/CN]; Pokfulam Road, Hong Kong (CN).

(72) Inventors: **CHOY, Chik Ho, Wallace**; Flat G, 9th Floor, 13 Block, Chevalier Garden, Ma On Shan, Shatin, Hong Kong (CN). **ZHANG, Hong**; R904A, 9th Floor, Morrison Hall, 109 Pokfulam Road, Hong Kong (CN).

(74) Agent: **CHINA PATENT AGENT (H.K.) LTD.**; 22/F., Great Eagle Center, 23 Harbour Road, Wanchai, Hong Kong (CN).

(81) Designated States *(unless otherwise indicated, for every kind of national protection available)*: AE, AG, AL, AM, AO, AT, AU, AZ, BA, BB, BG, BH, BN, BR, BW, BY, BZ, CA, CH, CL, CN, CO, CR, CU, CZ, DE, DK, DM, DO, DZ, EC, EE, EG, ES, FI, GB, GD, GE, GH, GM, GT, HN, HR, HU, ID, IL, IN, IR, IS, JP, KE, KG, KN, KP, KR, KZ, LA, LC, LK, LR, LS, LU, LY, MA, MD, ME, MG, MK, MN, MW, MX, MY, MZ, NA, NG, NI, NO, NZ, OM, PA, PE, PG, PH, PL, PT, QA, RO, RS, RU, RW, SA, SC, SD, SE, SG, SK, SL, SM, ST, SV, SY, TH, TJ, TM, TN, TR, TT, TZ, UA, UG, US, UZ, VC, VN, ZA, ZM, ZW.

(84) Designated States *(unless otherwise indicated, for every kind of regional protection available)*: ARIPO (BW, GH, GM, KE, LR, LS, MW, MZ, NA, RW, SD, SL, ST, SZ, TZ, UG, ZM, ZW), Eurasian (AM, AZ, BY, KG, KZ, RU, TJ, TM), European (AL, AT, BE, BG, CH, CY, CZ, DE, DK, EE, ES, FI, FR, GB, GR, HR, HU, IE, IS, IT, LT, LU, LV, MC, MK, MT, NL, NO, PL, PT, RO, RS, SE, SI, SK, SM, TR), OAPI (BF, BJ, CF, CG, CI, CM, GA, GN, GQ, GW, KM, ML, MR, NE, SN, TD, TG).

Published:
— *with international search report (Art. 21(3))*

(54) Title: AN ORGANOLEAD HALIDE PEROVSKITE FILM AND THE METHOD OF MAKING THE SAME

Figure 1

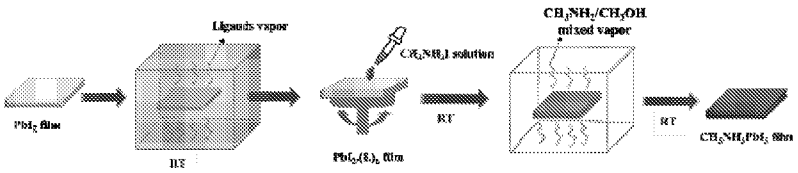

(57) Abstract: Methods for the all room-temperature fabrication of organolead halide perovskite films which are PbI_2 residue-free, have large grain-sizes, and are highly crystalline. All room-temperature fabrication of high-performance flexible perovskite solar cells are achieved by using such organolead halide perovskite films.

WO 2018/000294 A1

AN ORGANOLEAD HALIDE PEROVSKITE FILM AND THE METHOD OF MAKING THE SAME

Field of the Invention

[0001] The present invention relates to solar energy generation, and particularly to photovoltaic films and methods of making them.

Background of the Invention

[0002] Electricity is the most convenient and safe form of energy in our daily life, so the demand for electricity is gradually increasing as populations increase and industry develops. Therefore, direct generation of electricity from solar energy is of great interest because it is clean, renewable, abundant, and sustainable. However the power generation cost of solar cells is still more expensive than conventional fossil fuel, so there are limits on the widespread applications of solar cells. Accordingly, significant effort is being devoted to achieving a breakthrough in the development of cost-effective innovative solar cells by enhancing power conversion efficiency and reducing processing cost at the same time.

[0003] Recently innovative solar cells satisfying such criteria have been reported. These are the perovskite solar cells (PVSCs), which can be fabricated in an all solution process and which have a record power conversion efficiency of 22.1 % at 1 sun condition (100 mW/cm^2 AM 1.5G). However, the most advanced PVSCs still require a series of high-temperature sintering or annealing processes, which increase the fabrication cost and energy consumption. Furthermore, the high annealing temperature may be a concern for fabrication on flexible substrates. Flexible substrates enable the implementation of large scale portable and roll-to-roll fabrication. Since the cost and scalable capability are the key issues for their practical applications, low temperature and solution processed approaches for each layer of PVSCs are highly desirable.

Summary of the Invention

[0004] Embodiments of the present invention are drawn to methods of fabricating room-temperature solution-processed organolead halide perovskite films, as well as all room-temperature fabrication of high-performance bendable perovskite optoelectronic devices using such perovskite organolead halide films.

[0005] In one embodiment, a method of fabricating room-temperature solution-processed organolead halide perovskite film can include: forming PbX_2 solutions; forming PbX_2 films; drying the PbX_2 films naturally; forming $PbX_2.(L)_y$ film *in situ* by solid-gas reactions between ligand (L) vapor and PbX_2 film (X= I, Br, Cl, $C_2H_3O_2$) at room temperature; forming perovskite film by exposing the $PbX_2.(L)_y$ film to a solution of organic ammonium halide at room temperature; removing the resultant perovskite film from the organic ammonium halide solution; washing the perovskite film with isopropyl alcohol (IPA) and drying it naturally; exposing the as-formed perovskite film to a methylamine/alcohols gas mixture; removing the perovskite film from the methylamine/alcohols gas mixture; and drying the perovskite film.

[0006] In another embodiment, all room-temperature processed flexible PVSCs can be fabricated using the perovskite film described above as an absorber. The nanostructure-based NiO_x film and commercial electron transport materials such as ZnO, and fullerene (C_{60}) are used to form a hole transport layer (HTL) and an electron transport layer (ETL) in the all room-temperature solution-processed flexible PVSCs, respectively. The room-temperature processed electrode can be silver paste, gold paste, the inventor's recently invented silver nano-networks, etc.

Brief Description of the Drawings

[0007] The foregoing and other objects and advantages of the present invention will become more apparent when considered in connection with the following detailed description and appended drawings in which like designations denote like elements in the various views, and

wherein:

[0008] Figure 1 is a schematic of room-temperature fabrication of organolead halide perovskite films according to embodiments of the subject invention.

[0009] Figure 2(a) is a plot of UV-vis spectra of $PbI_2.(L)_x$ films; Figure 2(b) is a plot of X-ray powder diffraction (XRD) patterns of the $PbI_2.(L)_x$ films of Figure 2(a); Figure 2(c) is a graph of theoretically calculated interlayer distances of the $PbI_2.(L)_x$ films of Figure 2(a); Figure 2(d) is a top-view of scanning electron microscope (SEM) images of the pristine PbI_2 of Figure 2(a); Figure 2(e) is a top-view of SEM images of the $PbI_2.(Py)_2$ film of Figure 2(a); Figure 2(f) is a top-view of SEM images of the PbI_2.TBP film of Figure 2(a); Figure 2(g) is a top-view of SEM images of the $PbI_2.(DMSO)_2$ film of Figure 2(a); Figure 2(h) is a top-view of SEM images of the PbI_2.DMF film of Figure 2(a); Figure 2(i) is a top-view of SEM images of the $PbI_2.(DEA)_2$ film of Figure 2(a); Figure 2(j) is a transmission electron microscope (TEM) image of the PbI_2 of Figure 2(a); and Figure 2(h) is a TEM image of the PbI_2 of Figure 2(a).

[0010] Figure 3(a) is a plot of XRD patterns of perovskite films from different $PbI_2.(L)x$ films after immersion in CH_3NH_3I solution for 20 sec.; Figure 3(b) is a plot of UV-vis spectra of the perovskite films of Figure 3(a); Figure 3(c) is a top-view of the SEM images of the perovskite film from PbI_2 film; Figure 3(d) is a top-view of SEM images of perovskite films from $PbI_2.(Py)_2$ film; Figure 3(e) is a top-view of SEM images of perovskite films from PbI_2.TBP film; Figure 3(f) is a top-view of SEM images of perovskite films from $PbI_2.(DMSO)_2$ film; Figure 3(g) is a top-view of SEM images of perovskite films from PbI_2.DMF film; Figure 3(h) is a top-view of an SEM image of $PbI_2.(DEA)_2$ film after being dipped into CH_3NH_3I solution; Figure 3(i) is a plot of XRD patterns for the 110 reflection from the perovskite films of Figure 3(d) before and after recrystallization; Figure 3(j) is a top-view of SEM images of the perovskite films of Figure 3(d) after recrystallization; Figure 3(k) is a cross-sectional SEM image of the perovskite films of Figure 3(d) after recrystallization; and Figure 3(l) is a magnified image of the SEM image of Figure 3(k).

[0011] Figure 4(a) is a schematic of the all room-temperature solution-processed fabrication process for PVSCs according to an embodiment of the present invention; Figure 4(b) is a J-V curve of an all room-temperature solution-processed fabrication of $PbI_2.(Py)_2$-based PVSCs on an ITO glass substrate; Figure 4(c) is a plot of the photon-to-electron conversion efficiency (IPCE) spectra of the device of Figure 4(b); Figure 4(d) is a plot of photocurrent output and PCE at the maximum power point (0.88 V) for the device of Figure 4(b); Figure 4(e) is the PCE distribution histogram of $PbI_2.(Py)_2$-based PVSCs; Figure 4(f) is a plot of the PCE evolution of an encapsulated device of Figure 4(b) stored in ambient air (45~65% humidity, 20~28℃) for different numbers of days; and Figure 4(g) is J-V curves of a $PbI_2.(Py)_2$-based PVSCs measured under different scan directions.

[0012] Figure 5 is a J-V curve and the photograph (inserted) of a flexible PVSC on a polyethylene terephthalate (PET) substrate.

Detailed Description of Exemplary Embodiments of the Invention

[0013] The present invention relates to new approaches to fabrication of high-efficiency and flexible PVSCs, which can help to form a platform to leverage the development in green energy and flexible electronics. Regarding applications, the PVSCs have special advantages for use in new applications such as unmanned aerial vehicles—from airplanes to quadcopters and weather balloons—for environmental and industrial monitoring, rescue and emergency response, and tactical security applications.

[0014] Perovskite solar cells have drawn enormous attention because of their remarkably high efficiency and prospective low-cost fabrication. A new certificated efficiency of 22.10% has recently been achieved, and the theoretical limit of the PVSC efficiency has been estimated to be 31% based on the photon recycling effect through the detailed balance model. This makes them a very promising candidate to be used for next-generation photovoltaics.

[0015] Priority in the previous studies of PVSCs was given to improving their power

conversion efficiencies (PCEs) by optimizing device structure and developing new interface materials. However, most of the state-of-the-art PVSCs require a series of high-temperature sintering or annealing processes to fabricate efficient carrier-transport layers (e.g., TiO_2, PEDOT:PSS, NiO_x) and perovskite absorbers (e.g., $CH_3NH_3PbI_3$). Various and multi-step processing conditions in forming each layer in multilayered PVSCs increase the fabrication complexity and energy consumption, and thus the cost and energy payback time. In addition, the high annealing temperature may be a concern for fabrication on flexible substrates. More importantly, it has been reported that the film quality (crystallinity, purity) and morphology of perovskite films are depend on the thermal annealing temperature. For example, traditional approaches employ thermal annealing to remove the organic residue (e.g., high-boiling-point solvents) in precursors and to improve the crystallization of perovskite films. However, thermal annealing for extended periods is known to cause the decomposition of perovskite films, which degrades the device performance and stability. Since cost and scalability are among the critical issues for their practical applications, low temperature and solution-processed methods for each layer of PVSC are highly desirable. Meanwhile, there has still been very limited study on fully room-temperature solution-processed fabrication of PVSCs, which is challenging and desirable so as to enable large-scale, roll-to-roll manufacturing of perovskite-based photovoltaics.

[0016] Embodiments of the present invention are directed to methods of fabricating all room-temperature solution-processed organolead halide perovskite films, as well as all room-temperature fabrication of high-performance bendable perovskite solar cells (PVSC) using such organolead halide perovskite films. It is a scalable process and the $CH_3NH_3PbI_3$ film produced provides good film quality and smooth morphology.

[0017] The basic process for producing the film is shown in Figure 1. The first element of Figure 1 shows that first, the $PbI_2.(L)_x$ film is prepared in situ by solid-gas reactions:

$$PbI_2\ (solid) + x\,L\ (gas) \overset{25^{\circ}C}{\longleftrightarrow} PbI_2\ (L)_x\ (solid)$$

The ligand contains at least one component selected from pyridine ("Py"), 4-tert-butylpyridine

("TBP"), ethylene diamine ("DMSO"), N,N'-dimethylmethanaide ("DMF"), and dimethyl sulfoxide ("EDA").

[0018] Second, the high-purity perovskite film is produced by controllable ligand (L) exchange reactions:

$$PbI_2.(L)_x(solid) + CH_3NH_3I(liquid) \xrightarrow{25^{\circ}C} CH_3NH_3PbI_3(solid) + L(liquid)$$

[0019] Subsequently, the crystallinity of $CH_3NH_3PbI_3$ films can be further improved by introducing CH_3NH_2/CH_3CH_2OH mixed vapor treatment, again under room temperature. All room-temperature solution processed PVSCs can be fabricated with the configuration of ITO/NiO_x/ $CH_3NH_3PbI_3$ /C_{60}/Bis-C_{60}/Ag, where room-temperature solution-processed NiO_x nanostructure, C_{60}, and Bis-C_{60} surfactant as HTL, ETL, and interface layer, respectively

[0020] Methods according to the present invention provide a simple and low cost approach for the fabrication of high-quality perovskite films at room temperature. In one embodiment, a method of fabricating room-temperature solution-processed organolead halide perovskite film can include: forming PbX_2 solutions; forming PbX_2 films; drying the PbX_2 films naturally; forming $PbX_2.(L)_y$ film *in situ* by solid-gas reactions between ligand (L) vapor and PbX_2 film; forming perovskite film by exposing the $PbX_2.(L)_y$ film in a solution of organic ammonium halide at room temperature; removing the resultant perovskite film from the organic ammonium halide solution; washing the perovskite film with isopropyl alcohol (IPA) and drying it naturally; exposing the as-formed perovskite film in a methylamine/alcohols gas mixture; removing the perovskite film from the methylamine/alcohols gas mixture; and drying the perovskite film. The room temperature processed perovskite films exhibit a highly crystalline phase with strong (110) preferred orientation [X-ray diffraction (XRD) peak relative intensity: (110):(220):(330)=1:0.67:0.09] and large grain sizes (300-600nm; others <300nm). These properties can be easily measured by standard equipment such as X-ray diffraction (XRD) and scanning electron microscope (SEM). In many embodiments, no expensive or hi-tech equipment is required. Low cost materials can be used, and the energy required can also be low, leading to low power consumption. The process can be carried out at room temperature. No toxic by-

products are needed or generated during the process.

[0021] The PbX_2 can be PbI_2, $PbBr_2$, $PbCl_2$,$Pb(C_2H_3O_2)_2$ or a mixture thereof, although the present invention is not limited thereto.

[0022] The PbX_2 film can be formed by, for example, depositing a solution of PbX_2 on a substrate through, e.g., spin coating, drop casting, spray coating, Mayer rod techniques, and/or doctor blade techniques. The as-formed PbX_2 films are dried naturally without annealing. The dimensions of the PbX_2 films can be any suitable value known in the art. The dimension shown in the examples discuss herein are for exemplary purposes only and should not be construed as limiting. The solvent can be, for example, *N,N'*-dimethylmethanaide (DMF), dimethyl sulfoxide (DMSO), *N*-Methyl-2-pyrrolidone (NMP) or any combination thereof, although the present invention is not limited thereto.

[0023] The concentration of the PbX_2 solution can be in the range of about 0.05 to 1.50. For example, it can be any of the following values, about any of the following values, at least any of the following values, no more than any of the following values, or within any range having any of the following values as endpoints (all values are in millimolar (mM)), although the present invention is not limited thereto: 0.05, 0.10, 0.15, 0.20, 0.25, 0.30, 0.35, 0.40, 0.45, 0.50, 0.55, 0.60, 0.65, 0.70, 0.75, 0.80, 0.85, 0.90, 0.95, 1.0, 1.05, 1.10, 1.15, 1.20, 1.25, 1.30, 1.35, 1.40, 1.45, 1.50. For example, the concentration of PbI_2 within a DMF solution can be between 0.05 mM and 1.05 mM at room temperature. In a particular embodiment, the PbI_2 within a DMSO solution is between 0.05 mM and 1.30 mM.

[0024] Thanks to the two-dimensional structure of PbX_2, the interlayer spaces allow rapid intercalation of different guest molecules owing to the weak bonding between the two planes by *van der Waals*-type interactions, leading to the expansion of the interlayer distance along the *c* axis. Bearing this in mind, $PbX_2.(L)_y$ films are easily synthesized *in situ* by solid-gas reactions between PbX_2 films and chemical ligand (L) vapors at room temperature. The formation and composition of $PbX_2.(L)_y$ complexes can be confirmed from UV-vis spectra and XRD patterns.

[0025] The ligand for preparing the $PbX_2.(L)_y$ films can be pyridine (Py), 4-tert-butylpyridine (TBP), ethylene diamine (EDA), DMF, DMSO, or a mixture thereof, although the present invention is not limited thereto. The morphology and reactivity toward organic ammonium halide of the $PbX_2.(L)_y$ complexes can be determined by the value of *y* and the type of ligand. The value of *y* can be determined by the reaction time between PbX_2 and ligand vapors. The reaction time between PbX_2 and ligand vapors can be in the range of about 10 sec. to 1000 sec. For example, it can be, for example, any of the following values, about any of the following values, at least any of the following values, no more than any of the following values, or within any range having any of the following values as endpoints (all values are in seconds), although the present invention is not limited thereto: 10, 20, 30, 40, 50, 60, 70, 80, 90, 100, 110, 120, 130, 140, 150, 160, 170, 180, 190, 200, 210, 220, 230, 240, 250, 260, 270, 280, 290, 300, 350, 400, 450, 500, 550, 600, 650, 700, 750, 800, 850, 900, 950, or 1000.

[0026] The organic ammonium halide can be, for example, methylammonium iodide, methylammonium bromide, methylammonium chloride, formamidinium iodide, formamidinium bromide, formamidinium chloride, or a mixture thereof, although the present invention is not limited thereto.

[0027] The concentration of the organic ammonium halide can be in the range of about 0.03 to 0.50. For example, it can be any of the following values, about any of the following values, at least any of the following values, no more than any of the following values, or within any range having any of the following values as endpoints (all values are in millimolar (mM)), although the present invention is not limited thereto: 0.03, 0.04, 0.05, 0.06, 0.07, 0.08, 0.09, 0.10, 0.15, 0.20, 0.25, 0.30, 0.35, 0.40, 0.45 or 0.50. For example, the concentration of organic ammonium halide within an isopropyl alcohol (IPA), solution can be between 0.03 mM and 0.50 mM. In a particular embodiment, the organic ammonium halide is methylammonium iodide and the concentration of methylammonium iodide within an IPA solution is between 0.03 mM and 0.40 mM.

[0028] The immersing time of $PbX_2.(L)_y$ in organic ammonium halide can be in the range of

about 10 to 1000 sec. For example, it can be any of the following values, about any of the following values, at least any of the following values, no more than any of the following values, or within any range having any of the following values as endpoints (all values are in seconds), although the present invention is not limited thereto: 10, 20, 30, 40, 50, 60, 70, 80, 90, 100, 110, 120, 130, 140, 150, 160, 170, 180, 190, 200, 210, 220, 230, 240, 250, 260, 270, 280, 290, 300, 350, 400, 450, 500, 550, 600, 650, 700, 750, 800, 850, 900, 950, or 1000. For example, the immersing time of $PbX_2.(L)_y$ within a methylammonium iodide IPA solution can 10-60 seconds. In a particular embodiment, the $PbX_2.(L)y$ is $PbI_2(Py)_2$ and the immersing time of $PbI_2(Py)_2$ within methylammonium iodide IPA solution is 20 sec. or about 20 sec.

[0029] The step of drying the perovskite films can be carried out by any suitable process known in the art, including but not limited to blow drying, vacuum drying, air drying, or any combination thereof.

[0030] The alcohols in the step of methylamine/alcohols mixture treatment can be, for example, methanol, ethanol, IPA, or a mixture thereof, although the present invention is not limited thereto. The ratio of the methylamine to the alcohols can be in the range of about 1:20 to 20:1. For example, it can be any of the following values or about any of the following values (all ratios are by weight), although the present invention is not limited thereto: 1:20, 1:19, 1:18, 1:17, 1:16, 1:15, 1:14, 1:13, 1:12, 1:11, 1:10, 1:9, 1:8, 1:7, 1:6, 1:5, 1:4, 1:3, 1:2, 1:1, 2:1, 3:1, 4:1, 5:1, 6:1, 7:1, 8:1, 9:1, 10:1, 11:1, 12:1, 13:1, 14:1, 15:1, 16:1, 17:1, 18:1, 19:1, or 20:1. For example, the alcohol in methylamine/alcohols mixture can be ethanol. In a particular embodiment, the ratio of the methylamine to the ethanol is 1:3.

[0031] The duration of time of the treatment of the methylamine/alcohols gas mixture can be in the range of about 1 to 60. For example, it can be any of the following values, about any of the following values, at least any of the following values, no more than any of the following values, or within any range having any of the following values as endpoints (all values are in seconds), although the present invention is not limited thereto: 1, 2, 3, 4, 5, 6, 7, 8, 9, 10, 11, 12, 13, 14, 15, 16, 17, 18, 19, 20, 21, 22, 23, 24, 25, 26, 27, 28, 29, 30, 35, 40, 45, 50, 55, 60. For example, the

treatment duration can be 1-5 seconds for methylamine/ethanol gas mixture.

[0032] The features (molecular size, volatility, solubility, and coordination ability toward PbX_2 of the ligand have great impact on the formation of perovskite films. As for $PbX_2.(L)_y$ complexes, the conversion rate of PbX_2 to $PbX_2.(L)_y$ complex is controlled by the volatility of the ligand (see Table 1). Besides, the reactivity of the $PbX_2.(L)_y$ complexes toward organic ammonium halide is determined by the coordination ability of the ligands. Furthermore, the molecular size and solubility of the ligands will affect the morphology of the $PbX_2.(L)_y$ film. On one hand, the insertion of ligands into the interlayer space of the PbX_2 will cause volume expansion and thus a different morphology from the initial PbX_2 film at a nanometer scale. On the other hand, the solubility of PbX_2 in the ligands (see Table 1) is also an important factor. If the solubility of PbX_2 in the chemical ligands is too large, i.e. DMF (475 mg ml^{-1}) and DMSO (595 mg ml^{-1}), the morphological structure of the $PbX_2.(L)_y$ film will change a lot at a large scale (micrometer scale) due to the ligand vapors. On the contrary, the morphology of the final $PbX_2.(L)_y$ films (L= Py, TBP, and DEA) will not be changed at a large scale. In the process of perovskite film formation, the morphology of $PbX_2.(L)_y$ films and reactivity of the $PbX_2.(L)_y$ complexes toward organic ammonium halide are two key factors. The morphology of perovskite film is controlled by the morphology of $PbX_2.(L)_y$ films. The purity of perovskite is a result of the combining effects of the reactivity, conversion rate, and morphology of $PbX_2.(L)_y$ films.

[0033] Methods of the present invention can be carried out at room temperature and room pressure, i.e., at any suitable temperature and pressure present in a typical indoor setting. Advantageously, no toxic gases or chemicals are needed for the methods, and no toxic gases or chemicals are produced while the methods are carried out.

[0034] In another embodiment, all room-temperature processed flexible perovskite solar cells (PVSCs) are fabricated using the perovskite film described above as an absorber. The nanostructure-based NiO_x film and commercial electron transport materials such as ZnO, and fullerene (C_{60}) are used to form a hole transport layer (HTL) and an electron transport layer (ETL) in the all room-temperature solution-processed flexible PVSCs, respectively. It would be

understood by a person skilled in the art that the electron transport materials herein are not limited to these examples, and instead they can be any materials that are suitable for such electron transport materials. The room-temperature processed electrode can be silver paste, gold paste, the inventors' recently invented silver nano-networks, etc. It would be understood by a person skilled in the art that the electrode materials herein are not limited to these examples, and instead the electrode can be fabricated from any materials that are suitable for such electrode. The substrate can be any suitable substrate known in the art, including but not limited to, indium tin oxide (ITO) transparent conductive glass, fluorine doped tin oxide (FTO) glass, metal foils, and a flexible transparent conductive substrate.

[0035] Figure 4(a) is a schematic of an all room-temperature solution-processed fabrication of PVSCs according to an embodiment of the present invention with the resulting product shown at the last step. In particular, Figure 4(a) shows a series of continuous processing steps. Firstly, ITO-coated glass substrates were cleaned and then ultraviolet-ozone treated for 20 min. Then, the NiO_x nanoparticles aqueous ink (20 mg/mL in deionized water) was spin-coated onto pre-cleaned ITO glass to form nanostructured NiO_x films. The resultant NiO_x films are used to fabricate devices without an annealing process or other treatments. After forming perovskite films based on different ligands, the C_{60} (20 mg/ml dissolved in dichlorobenzene) and Bis-C_{60} surfactant (2 mg/mL in IPA) are then sequentially deposited by spin coating at 1,000 rpm for 60 sec. and 3,000 rpm for 30 sec., respectively. Finally, the device is completed with the evaporation of Ag contact electrodes (120 nm) through a shadow mask. The active area of this electrode was fixed at 6 mm^2. All devices were fabricated in a glove box.

[0036] Figure 4(b) is a J-V curve of an all room-temperature solution-processed fabrication of $PbI_2.(Py)_2$-based PVSCs on an ITO glass substrate as shown at the last step in Figure 4(a). Figure 4(c) is a plot of IPCE spectra of the device of Figure 4(a). Figure 4(d) is a plot of the photocurrent output and PCE at the maximum power point (0.88 V) for the device of Figure 4(a). Figure 4(e) is the PCE distribution histogram of $PbI_2.(Py)_2$-based PVSCs of Figure 4(a). Figure 4(f) is a plot of the PCE evolution of an encapsulated device of Figure 4(a) stored in ambient air

(45~65% humidity, 20~28°C) for different numbers of days. Figure 4(g) is J-V curves of a

$PbI_2.(Py)_2$-based PVSCs device of Figure 4(a) measured under different scan directions.

[0037] The thickness of perovskite film can be in the range of about 50 to 1000 nanometers. For example, it can be any of the following values, no more than any of the following values, at least any of the following values, or within any range having any of the following values as endpoints (all values are in nanometers), although the present invention is not limited thereto: 50, 100, 150, 200, 250, 300, 350, 400, 450, 500, 550, 600, 650, 700, 750, 800, 850, 900, 950 or 1000. For example, the perovskite film thickness of high-performance PVSCs is around 300 nanometers.

[0038] In many embodiments, more than one PbX_2 or organic ammonium halide can be present in some or all of the perovskite films.

[0039] Following are examples that illustrate procedures for practicing the invention. These examples should not be construed as limiting. All percentages are by weight and all solvent mixture proportions are by volume unless otherwise noted.

EXAMPLE 1

[0040] The PbI_2 precursor was prepared by dissolving 450mg PbI_2 powder in 1ml DMF, then spin coating it on a substrate at 4000 rpm for 60 sec. After the PbI_2 films were totally dried, the resultant PbI_2 films were treated by different chemical ligand vapors for different times to form $PbI_2.(L)_x$ films. The resulting $PbI_2.(L)_x$ films were then dipped in a solution of 15 mg methylammonium iodide per ml IPA for 20 sec., rinsed with IPA and dried with N_2 gas. The crystallization of the resulting methylammonium lead iodide raw films was improved by treatment with a methylamine/methanol gas mixture for 1-5 sec. The features of these ligands and

$PbI_2.(L)_x$ films are shown in Table 1.

Table 1

The basic chemical properties of different chemical ligands

Ligand	Boiling point (°C)	PbI_2 solubility (mg/ml)[a]	$PbI_2.(L)_x$ conversion rate(s)[b]	PbI_2/L coordination ratio[c]	Theoretically calculated interlayer distance of $PbI_2.(L)_x$ (Å)
-	-	-	-	–	6.918[d]
Py	115	<5	100	1:2	8.598
TBP	197	148	300	1:1	15.152
DMSO	189	595	140	1:2	8.437
DMF	153	475	50	1:1	9.196
EDA	116	<5	50	1:2	-

[0041] a. PbI_2 (99%) was purchased from Sigma-Aldrich. The solubility test was conducted at room temperature (25 °C). b. The progress of chemical reactions was monitored by UV-vis-spectra. c. The data were estimated by TGA. d. Theoretically calculated interlayer distance of PbI2

[0042] The formation and composition of PbI2.(L)x complexes can be confirmed from UV-vis spectra (Figure 2(a)). Owing to the high volatility of DMF and EDA with boiling points of 153 °C and 116 °C, respectively, the yellow-colored PbI2 rapidly changed to colorless in the visible region upon treatment by their vapors for 50 seconds (The conversion rate was monitored by UV-vis spectra). The formation of colorless PbI2.(Py)2 and PbI2.(DMSO)2 took 100 sec. and 140 sec., respectively. The complete transformation of PbI2 into the PbI2.TBP complex was relatively slow (300 sec.) due to the high boiling point (197 °C) of TBP. Besides, the formation

of PbI2.(L)x was further confirmed by an X-ray powder diffraction (XRD) pattern (Figure 2(b)). After the initial PbI2 film was treated by the ligands vapor (except for DEA), it not only exhibited Bragg peaks associated with PbI2 crystal (001) planes at 12.55, but also other new peaks at low angles, indicating the formation of PbI2.(L)x complex. Meanwhile, the appearance of XRD peaks at low angles indicates that the PbI2.(L)x complex has longer interlayer distances along the c axis (see Figure 2(c)), which is beneficial to the substitution of CH3NH3I. See, W. S. Yang, J. H. Noh, N. J. Jeon, Y. C. Kim, S. Ryu, J. Seo, S. I. Seok, *Science* 2015, 348, 1234 ("Yang") and N. J. Jeon, J. H. Noh, Y. C. Kim, W. S. Yang, S. Ryu, S. I. Seok, *Nat Mater.* 2014, 13, 897 ("Jeon"), both of which are incorporated herein by reference in their entirety. However, the PbI2 coordinated with EDA tend to form a stable stoichiometric complex PbI2.(DEA)2, which showed a totally different XRD patterns from PbI2.

[0043] The formation process of $PbI_2.(L)_x$ films was revealed by SEM images as shown in Figures 2(d)-2(i). It should be noted that the untreated PbI_2 forms dense and layered crystals (Figure 2(d)), which has been demonstrated to be detrimental to the complete conversion of PbI_2. See, H. Zhang, J. Mao, H. He, D. Zhang, H. L. Zhu, F. Xie, K. S. Wong, M. Grätzel, W. C. H. Choy, *Adv. Energy Mater.* **2015**, 5, 1501354 ("Zhang") and J. Burschka, N. Pellet, S.-J. Moon, R. Humphry-Baker, P. Gao, M. K. Nazeeruddin and M. Grätzel, *Nature* **2013**, 499, 316 ("Burschka"), both of which are incorporated herein by reference in their entirety. Interestingly, the insertion of ligands into the interlayer spaces of PbI_2 brought a huge morphological change for $PbI_2.(L)_x$ films, which verified the hypothesis above. As shown in Figure 2(e), $PbI_2.(Py)_2$ complex shown a uniform and nanoporous morphology, which also has been verified by TEM images. When treated by Py vapor, the bulk PbI_2 nanocrystals (Figure 2(j)) changed to porous $PbI_2.(Py)_2$ nanocrystals (Figure 2(k)). While PbI_2.TBP complex was nonporous, its morphology was non-uniform in large scale (Figure 2(f)). The $PbI_2.(DMSO)_2$ film was also porous and formed by stacked small nano-sheets (Figure 2(g)). Notably, the process of forming PbI_2.DMF film underwent remarkable structure changes over this time period, exhibiting a coarsening of crystals with micrometer size and voids occur (Figure 2(h)). The $PbI_2.(DEA)_2$ film was dense with some cracks (Figure 2(i)).

[0044] The features of the ligands also have great impact on the film quality and morphology of perovskite films. Herein, the perovskite films were fabricated by dipping the as-formed $PbI_2.(L)_x$ films into methylammonium iodide IPA solution (15 mg ml^{-1}) for 20 seconds at room temperature as shown in Figure 1. As expected from the conversion of $PbI_2.(L)_x$ to methylammonium lead iodide perovskite films, the ligand molecules intercalated in PbI_2 will be replaced by external methylammonium iodide because of its higher affinity toward PbI_2 compared to ligands. Therefore, the reactivity of $PbI_2.(L)_x$ toward methylammonium iodide has great impact on the perovskite film's formation, which is confirmed by UV-vis spectra and XRD. Notably, for the $PbI_2.(DEA)_2$ complex, there is no clear light absorption (Figure 3(a)) and XRD peaks of perovskite (Figure 3(b)), which indicate that the affinity of DEA toward PbI_2 is higher than that of MAI, and thus the DEA molecule is not exchanged by methylammonium iodide to form perovskite crystals. Interestingly, $PbI_2.(Py)_2$ film is rapidly converted into perovskite without clear PbI_2 residue. While pristine PbI_2 and other $PbI_2.(L)_x$ complexes (L= TBP and DMF) are incompletely converted into perovskite with a large amount of PbI_2 residue, but no $PbI_2.(L)_x$ residue, which can be confirmed by the XRD patterns (Figure 3(b)). However, owing to the strong affinity of DMSO toward PbI_2, $PbI_2.(DMSO)_2$ residue is still detected.

[0045] Figures 3(c)-3(h) show the top-view SEM images of methylammonium lead iodide perovskite films from different $PbI_2.(L)_x$ complexes. As expected the morphology of perovskite films depends on their starting PbI_2 film in the two-step dipping method. See the Zhang and Burschka articles with P. Gao, M. Gratzel, M. K. Nazeeruddin, *Energy Environ. Sci.* **2014** 7, 2448 ("Gao") and Y. Wu, A. Islam, X. Yang, C. Qin, J. Liu, K. Zhang, W. Peng, L. Han, *Energy Environ. Sci.* **2014**, 7, 2934 ("Wu"), both of which are incorporated herein by reference in their entirety. The perovskite films prepared from pristine PbI_2 and $PbI_2.(L)_x$ complex (L= TBP, DMSO, and DMF) are rough with small grains, voids and cracks. Notably, the perovskite film prepared from $PbI_2.(Py)_2$ complex exhibits a uniform/smooth morphology and hundred nanometer sized grains. Figure 3(i) shows the XRD intensity for the as-prepared perovskite films and 'recrystallized' perovskite films under identical measurement conditions, showing an over 200-fold increase in the counts after recrystallization. This change is indicative of higher degree

of crystallinity and texture in the recrystallized perovskite film. As shown in Figures 3(j)-3(l), the top-view SEM images illustrate that the recrystallized perovskite films are more ultra-smooth with few gain boundaries, which are similar to that prepared from thermal annealing process.

EXAMPLE 2

[0046] All room-temperature processed PVSCs on ITO glass can be fabricated using the perovskite film described above as an absorber. The nanostructure-based NiO_x film and commercial electron transport materials such as fullerene (C_{60}) are used to form a hole transport layer (HTL) and an electron transport layer (ETL) in the all room-temperature solution-processed PVSCs, respectively.

[0047] The photovoltaic parameters of PVSCs fabricated form different PbI_2.(L)x complexes are summarized in Table 2. The results in Table 2 reveal that PVSC performances depend on the selection of chemical ligands. The performance of control perovskite (prepared from pristine PbI_2 film) is very poor and the average PCE is only 1.29%. The use of PbI_2.$(Py)_2$ complexes significantly improves photovoltaic performances and the overall average PCE dramatically increases to 15.80%. The improvement predominantly lies in the increased Jsc (from 2.17 to 22.14 mA cm^{-2}), which is attributed to the highly crystalline and pure perovskite films. The PbI_2.TBP and PbI_2.$(DMSO)_2$ complexes also provide an improvement in photovoltaic performances, yielding an average PCE of 11.45% and 9.61%, respectively. However, owing to the non-uniform and impure perovskite film with many pinholes, the PbI_2.DMF-based device have a low Voc of 0.85V, a Jsc of 16.30 mA cm^{-2} and a FF of 0.59, resulting in a relatively bad PCE of 8.17%. Notably, owing to the uniform perovskite crystals, the PbI_2.$(DEA)_2$-based device depicts no photovoltaic performance.

Table 2

The photovoltaic parameters of PVSCs fabricated from different PbI_2.$(L)_x$ complexes

Sample	J_{sc} (mA/cm^2)	V_{oc} (V)	FF	PCE (%)[a]
PbI_2	2.17±0.13	0.92±0.01	0.65±0.01	1.29±0.14
$PbI_2.(Py)_2$	22. 17±0. 42	0. 99±0. 02	0. 72±0. 02	15. 80±0. 72
$PbI_2.TBP$	17. 56±0. 45	1. 02±0. 02	0. 64±0. 01	11. 45±0. 51
$PbI_2.(DMSO)_2$	17. 02±0. 35	0. 96±0. 01	0. 59±0. 02	9. 61±0. 32
$PbI_2.DMF$	16. 30±0. 55	0. 85±0. 02	0. 59±0. 02	8. 17±0. 45
$PbI_2.(DEA)_2$	-	-	-	-

a) The statistics are determined from 15 devices.

[0048] Further improving the crystallinity of the perovskite films prepared form $PbI_2.(Py)_2$ complexes by methylamine/methanol gas mixture treatment for 1-5 sec., the best device based on the recrystallized perovskite film exhibited a Jsc of 22.60 mA cm^{-2}, a Voc of 1.05 V and an FF of 0.721, corresponding to a PCE of 17.10% as shown in Figure 4(b). The photon-to-electron conversion efficiency (IPCE) spectrum is shown in Figure 4(c), which is consistent with the Jsc from the current density-voltage (J-V) curves. Meanwhile, the stabilized power output with time was also investigated (Figure 4(d)). The photocurrent stabilizes within seconds to approximately 19.4 mA cm^{-2}, yielding a stabilized power conversion efficiency of 17.07%, measured after 100 sec. In order to investigate the reproducibility of the PVSCs, 30 separate devices were fabricated and tested. The histograms of the device efficiencies are presented in Figure 4(e). Approximately 85% of the cells show PCE over 15%. Besides, Figure 4(f) shows the air stability of the devices fabricated by this room temperature technique. The encapsulated device demonstrated good stability over a period of 1000 hours and maintained over 95% of its initial efficiency. To better understand the hysteresis of our PVSCs, the devices were measured under different scan directions and scan rates (Figure 4(g)). Notably, the room temperature processed devices

exhibited negligible hysteresis, which should be due to the highly crystalline perovskite films and the fullerene effect. See (a) Y. Zhao, C. Liang, H. Zhang, D. Li, D. Tian, G Li, X. Jing, W. Zhang, W. Xiao, Q. Liu, F. Zhang, Z. He, *Energy Environ. Sci.* **2015**, 8, 1256; (b) H.-S. Kim, N.-G Park, *J. Phys. Chem. Lett.* **2014**, 5, 2927; and (c) Y. Shao, Z. Xiao, C. Bi, Y. Yuan, J. Huang, *Nat. Commun.* **2014**, 5, 5784, each of which is incorporated herein by reference in their entirety.

EXAMPLE 3

[0049] By taking advantage of the room temperature techniques, flexible PVSCs utilizing ITO/PET as the conductive transparent electrode can be fabricated. Figure 5 shows the J-V curve of the PVSCs using flexible ITO/PET substrates under AM 1.5G irradiation and a photograph of a flexible PVSCs. The best flexible PVSC exhibits a Voc of 0.82V, a Jsc of 18.99 mA cm^{-2} and an FF of 0.73, corresponding to a high PCE of 11.42%, which is the highest PCE of flexible PVSCs fabricated by low temperature techniques.

[0050] Furthermore, in comparison to the previous studies on room temperature fabrication of PVSCs, the cells of the present invention are more efficient. See, D. Liu, T. L. Kelly, *Nat. Photon.* **2014**, 8, 133; U. Bansode, R. Naphade, O. Game, S. Agarkar, S. Ogale, *J. Phys. Chem. C* **2015**, 119, 9177 and Y. Chen, Y. Zhao, Z. Liang, *Chem. Mater.* **2015**, 27, 1448, each of which is incorporated herein by reference in their entirety.

[0051] What is more important, the Jsc of the present PVSCs is higher by ~1-2 mA cm^{-2} as compared to previous studies. The Jsc value of 21-23 mA cm^{-2} is closer to that of the champion cells with conventional device configuration based on $TiO_2/CH_3NH_3PbI_3$/spiro-OMeTAD. See, N. Ahn, D.-Y. Son, I.-H. Jang, S. M. Kang, M. Choi, N.-G Park, *J. Am. Chem. Soc.* **2015**, 137, 8696, which is incorporated herein by reference in their entirety.

[0052] It should be understood that the examples and embodiments described herein are for illustrative purposes only and that various modifications or changes in light thereof will be suggested to persons skilled in the art and are to be included within the spirit and purview of this

application and the scope of the appended claims. In addition, any elements or limitations of any invention or embodiment thereof disclosed herein can be combined with any and/or all other elements or limitations (individually or in any combination) or any other invention or embodiment thereof disclosed herein, and all such combinations are contemplated as being within the scope of the invention without limitation thereto.

CLAIMS

We claim:

1. A method of room-temperature fabrication of organolead halide perovskite films, the method comprising the steps of:

forming PbX_2 solutions;

forming PbX_2 films at room temperature from the PbX_2 solutions;

drying the formed PbX_2 films naturally;

forming $PbX_2.(L)_y$ film *in situ* by solid-gas reactions between ligand (L) vapor and the dried PbX_2 film at room temperature;

forming perovskite film by exposing the formed $PbX_2.(L)_y$ film to a solution of organic ammonium halide at room temperature;

removing resultant perovskite film from the solution of organic ammonium halide;

washing the removed resultant perovskite film with isopropyl alcohol (IPA);

drying the washed perovskite film naturally;

exposing the dried perovskite film to a methylamine/alcohols gas mixture;

removing perovskite film from the methylamine/alcohols gas mixture; and

drying the removed perovskite film.

2. The method according to claim 1, wherein the step of forming PbX_2 films involves depositing the PbX_2 solutions on a substrate by one of spin coating, drop casting, spray coating, Mayer rod techniques, or doctor blade techniques.

3. The method according to claim 1, wherein the PbX_2 can be selected from the group of PbI_2, $PbBr_2$, $PbCl_2$, $Pb(C_2H_3O_2)_2$ or an alloy thereof.

4. The method according to claim 1, wherein the concentration of the PbX_2 solution is in a range of from 0.05 in millimolar to 1.50 millimolar.

5. The method according to claim 1, wherein the ligand for forming the $PbX_2.(L)_y$ films is selected from the group consisting of pyridine, 4-*tert*-butylpyridine, ethylene diamine, *N,N'*-dimethylmethanaide, dimethyl sulfoxide, and an alloy thereof.

6. The method according to claim 1, wherein the ratio of the PbX_2 film to the ligand can be determined by reaction time between the dried PbX_2 film and ligand vapor, and wherein the reaction time is in a range of from 10 seconds to 100 seconds.

7. The method according to claim 1, wherein the organic ammonium halide is selected from the group consisting of methylammonium iodide, methylammonium bromide, methylammonium chloride, formamidinium iodide, formamidinium bromide, formamidinium chloride, and an alloy thereof, and wherein the concentration of the organic ammonium halide is in a range from 0.03 millimolar to 0.50 millimolar.

8. The method according to claim 1, wherein the exposure time of $PbX_2.(L)_y$ in the solution of organic ammonium halide is in a range from 10 seconds to 1000 seconds.

9. The method according to claim 1, wherein the alcohols in the step of exposing the dried perovskite film to a methylamine/alcohols gas mixture are selected from the group consisting of methanol, ethanol, IPA, and an alloy thereof, and wherein the ratio of the methylamine to the alcohols is in a range from 1:20 to 20:1.

10. The method according to claim 1, wherein the duration of time of step of exposing the dried perovskite film to a methylamine/alcohols gas mixture is in a range from 1 second to 60 seconds.

11. The method according to claim 1, wherein the organolead halide perovskite films exhibit a highly crystalline phase with strong (110) preferred orientation [X-ray diffraction (XRD) peak relative intensity: (110):(220):(330)=1:0.67:0.09] and large grain sizes (300-600nm; others <300nm).

12. A method of all room-temperature solution-processed fabrication of flexible perovskite solar cells, the method comprising:

depositing a formation solution comprising NiO_x nanoparticles dissolved therein on a flexible transparent conductive substrate, such that the NiO_x nanoparticles are well-packaged on the substrate to form a nanostructured NiO_x; and

fabricating the organolead halide perovskite films by the method according to any one on claims 1-11; and

depositing the electron transport layer on the organolead halide perovskite films; and

depositing conductive electrode on the electron transport layer.

13. The method according to claim 12, wherein the thickness of each of the organolead halide perovskite films is in a range from 50 nanometers to 1000 nanometers.

14. An all room-temperature solution-processed flexible perovskite solar cells fabricated by the methods according to claim 12 or 13.

15. A flexible perovskite solar cell comprising:

a flexible transparent conductive substrate;

a perovskite film acting as an absorber and located on the substrate;

an electron transport layer on the perovskite film; and

a conductive electrode on the electron transport layer;

wherein the perovskite film exhibits a highly crystalline phase with strong (110) preferred orientation and large grain sizes.

Figure 1

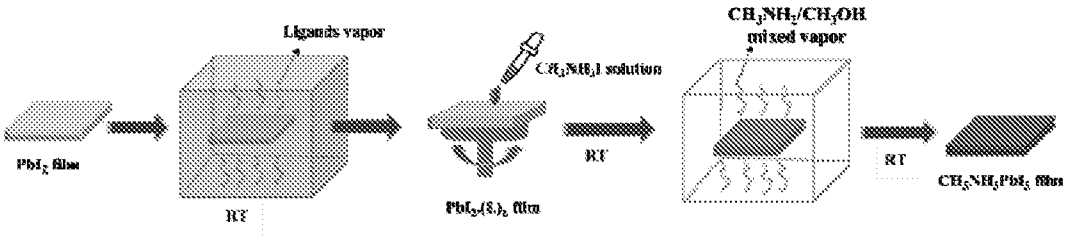

Figure 2

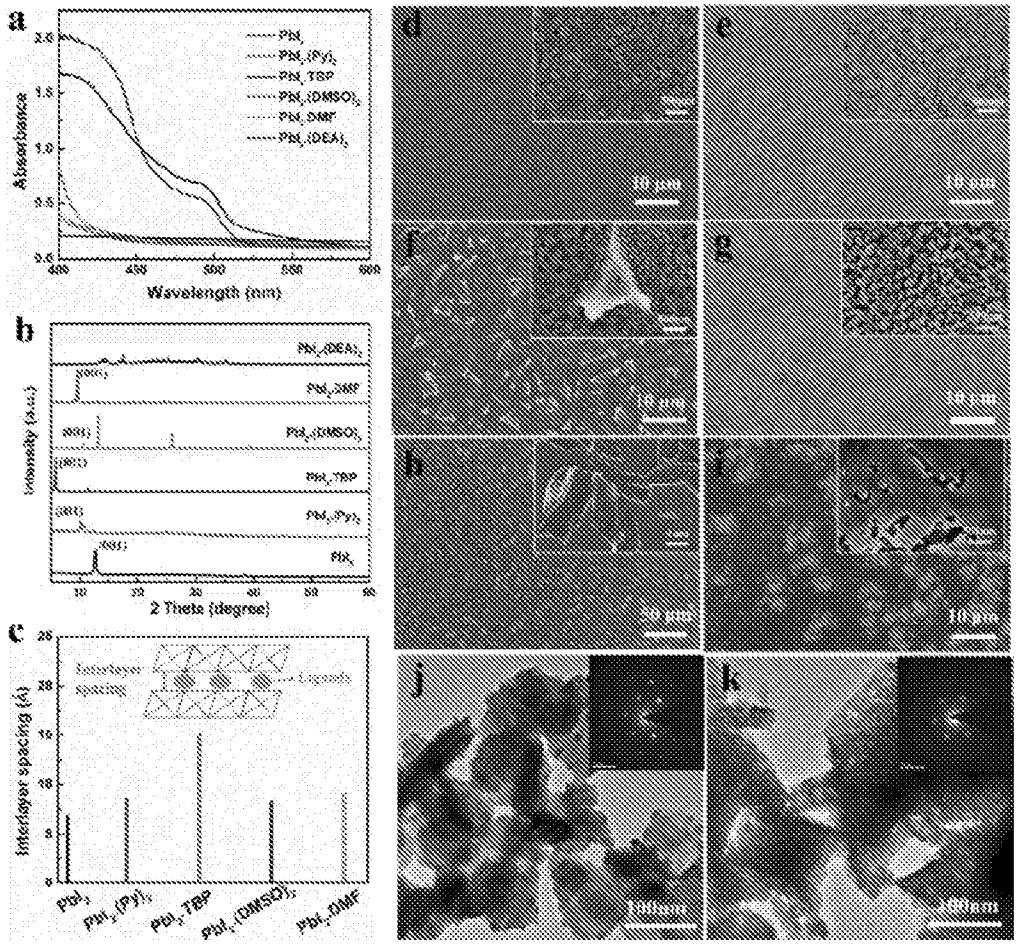

Figure 3

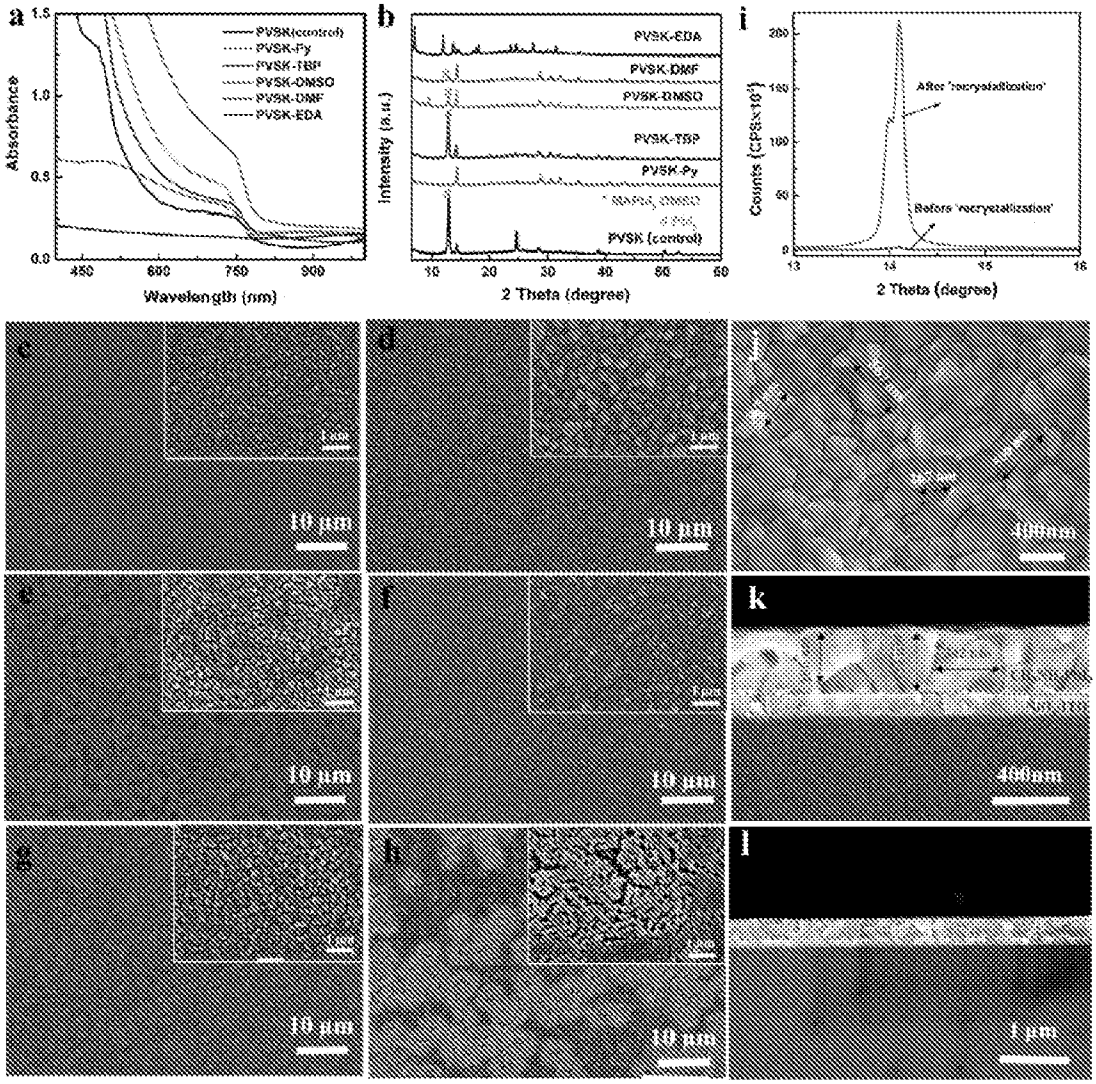
a
Absorbance
Wavelength (nm)
PVSK(control)
PVSK-Py
PVSK-TBP
PVSK-DMSO
PVSK-DMF
PVSK-EDA
b
Intensity (a.u.)
2 Theta (degree)
PVSK-EDA
PVSK-DMF
PVSK-DMSO
PVSK-TBP
PVSK-Py
PVSK (control)
i
Counts (CPS)
2 Theta (degree)
After recrystallization
Before recrystallization
c
d
e
f
g
h
j
k
l
10 μm
400nm
1 μm

Figure 4

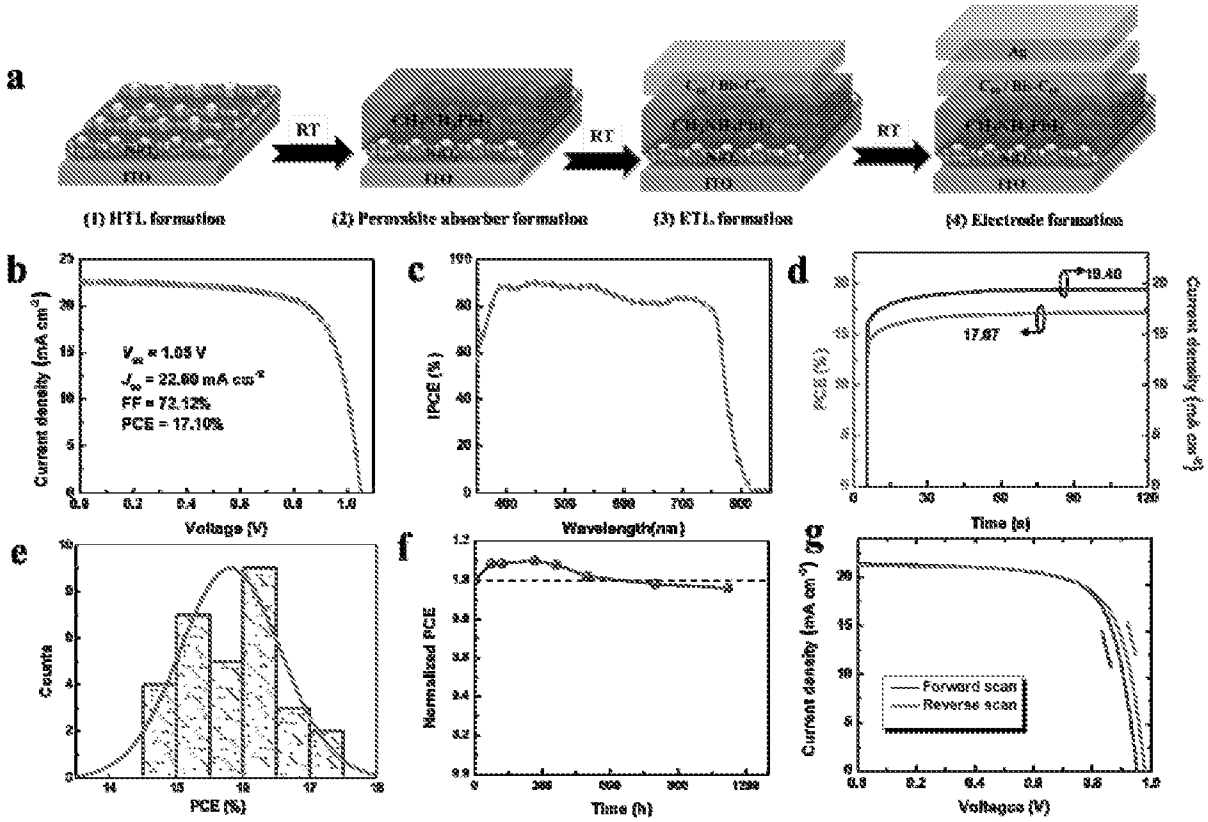
a
RT
RT
RT
(1) HTL formation
(2) Perovskite absorber formation
(3) ETL formation
(4) Electrode formation
b
Current density (mA cm-2)
Voltage (V)
c
IPCE (%)
Wavelength(nm)
d
Time (s)
e
Counts
PCE (%)
f
Normalized PCE
Time (h)
g
Current density (mA cm-2)
Voltage (V)
Forward scan
Reverse scan

Figure 5

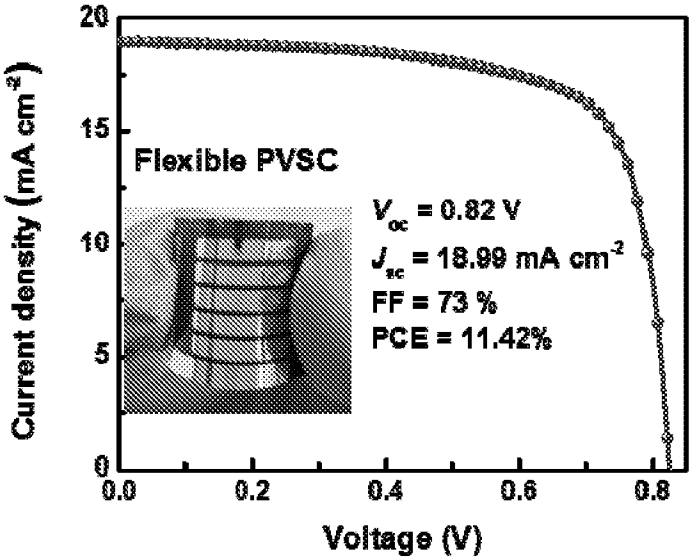
Current density (mA cm^{-2})
Voltage (V)
Flexible PVSC
V_{oc} = 0.82 V
J_{sc} = 18.99 mA cm^{-2}
FF = 73 %
PCE = 11.42%
0
5
10
15
20
0.0
0.2
0.4
0.6
0.8

INTERNATIONAL SEARCH REPORT

International application No.
PCT/CN2016/087831

A. CLASSIFICATION OF SUBJECT MATTER

H01L 31/032(2006.01)i; H01L 31/18(2006.01)i

According to International Patent Classification (IPC) or to both national classification and IPC

B. FIELDS SEARCHED

Minimum documentation searched (classification system followed by classification symbols)

H01L

Documentation searched other than minimum documentation to the extent that such documents are included in the fields searched

Electronic data base consulted during the international search (name of data base and, where practicable, search terms used)

CNTXT,CNABS,DWPI,SIPOABS,VEN:halide, perovskite, solar, cell, Pb, organic , organolead, large, grain, room, temperature

C. DOCUMENTS CONSIDERED TO BE RELEVANT

Category*	Citation of document, with indication, where appropriate, of the relevant passages	Relevant to claim No.
X	US 2015287852 A1 (LEUNG ET AL.) 08 October 2015 (2015-10-08) description, paragraphs [0059] to [0062] and figure 2	15
A	CN 103996749 A (UNIV SHANXI) 20 August 2014 (2014-08-20) the whole document	1-15
A	CN 104934503 A (UNIV LIAONING TECHNOLOGY) 23 September 2015 (2015-09-23) the whole document	1-15
A	CN 104966763 A (UNIV DALIAN TECHNOLOGY) 07 October 2015 (2015-10-07) the whole document	1-15
A	CN 105355724 A (UNIV NINGBO) 24 February 2016 (2016-02-24) the whole document	1-15
A	CN 105355794 A (SHENZHEN HONGKONG PRODN & RES BASE) 24 February 2016 (2016-02-24) the whole document	1-15

☐ Further documents are listed in the continuation of Box C. ☑ See patent family annex.

* Special categories of cited documents:

"A" document defining the general state of the art which is not considered to be of particular relevance

"E" earlier application or patent but published on or after the international filing date

"L" document which may throw doubts on priority claim(s) or which is cited to establish the publication date of another citation or other special reason (as specified)

"O" document referring to an oral disclosure, use, exhibition or other means

"P" document published prior to the international filing date but later than the priority date claimed

"T" later document published after the international filing date or priority date and not in conflict with the application but cited to understand the principle or theory underlying the invention

"X" document of particular relevance; the claimed invention cannot be considered novel or cannot be considered to involve an inventive step when the document is taken alone

"Y" document of particular relevance; the claimed invention cannot be considered to involve an inventive step when the document is combined with one or more other such documents, such combination being obvious to a person skilled in the art

"&" document member of the same patent family

Date of the actual completion of the international search	Date of mailing of the international search report
14 March 2017	**31 March 2017**

Name and mailing address of the ISA/CN	Authorized officer
STATE INTELLECTUAL PROPERTY OFFICE OF THE P.R.CHINA **6, Xitucheng Rd., Jimen Bridge, Haidian District, Beijing 100088** **China**	**WANG,Yibing**
Facsimile No. **(86-10)62019451**	Telephone No. **(86-10)62411584**

INTERNATIONAL SEARCH REPORT
Information on patent family members

International application No.
PCT/CN2016/087831

Patent document cited in search report	Publication date (day/month/year)	Patent family member(s)	Publication date (day/month/year)
US 2015287852 A1	08 October 2015	None	
CN 103996749 A	20 August 2014	CN 103996749 B	10 February 2016
CN 104934503 A	23 September 2015	None	
CN 104966763 A	07 October 2015	None	
CN 105355724 A	24 February 2016	None	
CN 105355794 A	24 February 2016	None	